# Dynamical edge effect factor determination for building components thermal characterization under outdoor test conditions in a PASLINK Test Cell: A methodological proposal.

C. García-Gáfaro *, C. Escudero-Revilla, I. Flores-Abascal, A. Erkoreka-González, K. Martín-Escudero,

ENEDI Research Group, Faculty of Engineering of Bilbao, University of the Basque Country (UPV/EHU), Plaza Ingeniero Torres Quevedo1, 48013 Bilbao, Spain

*e-mail: carlos.garciaga@ehu.eus

Phone: + (34) 94 601 8214, Fax: + (34) 94 601 4283

## Abstract

The thermal characterization of building components in dynamic exterior conditions is crucial for understanding their actual performance, particularly if they are passive or active solar elements. In this respect the PASLINK methodology has stood out as an effective technique for outdoor testing due to its level of development and precision. It is based on the use of calibrated test cell with interior walls covered by heat flow meters. The accurate determination of the heat flow through the envelope of the cell is essential for the subsequent thermal analysis of the passive/active solar component under test.

Although the walls of a PASLINK cell have a high thermal resistance and minimal thermal bridges, a higher heat flux is inevitable near the inner corners because of the edge effects. This variation is partially detected by heat flow meters, requiring correction factors accordingly named 'edge effect factors'. Additional heat flow meters strategically arranged in some interior corners are used to determine these factors in a calibration test. The factors calculated this way are used as invariable values in subsequent cell tests. However, the skill and criteria of the staff conducting the calibration test are fundamentals, and human errors can affect this process.

This proposal outlines a more objective and reliable new methodology to determine edge effect correction factors. It is based on applying correlations of instantaneous readings of heat flow meters. These correlations are obtained in an initial PASLINK calibration test but are valid for all subsequent tests. The factors calculated this way depend on instantaneous test readings, and for this reason they are dynamic values perfectly adapted to each test.

The calibration test of the cell called EGUZKI, located in Vitoria-Gasteiz (Northern Spain), is used to demonstrate the validity of the proposed method. With the current PASLINK calibration test methodology the calibrated cell obtains 13% of measurement error, while the new dynamic methodology proposed reduces this error to 6%.

Although this new methodology is determined in the context of a PASLINK test cell, it is an extensive method applicable to the correction of heat flow measurement affected by edge effects in general.

## A Keywords

Outdoor Test Cells / PASLINK / Dynamic Testing / Heat Flow Measurement Accuracy / Edge Factor / Border Thermal Bridge Characterization.

## B Nomenclature

| | | |
|---|---|---|
| $A(i); A(j)$ | Area covered by HFS-Tiles group (i) or (j) respectively | [$m^2$] |
| $F_c$ | Edge effect factor, ratio between actual to measured heat flow at edge, in the edge effect zone | [Adimensional] |
| $F_{c(T1)}, F_{c(T2)}, F_{c(T3)}$ | Edge effect factor for typologies 1, 2 and 3 respectively. | [Adimensional] |
| $F_{c\_t}$ | Total calibration factor of the cell | [Adimensional] |
| G1, G2... G21 | Group of HFS-Tiles connected in series, covering a specific area | [Adimensional] |
| $L$ | Length of edge zone measured by Tiles or Multi-Tiles in the edge | [m] |
| $L^{2D}$ | Thermal coupling coefficient obtained from 2D simulation, according to EN ISO 10211:2012 standard. | [W/m·K] |
| $n_{tr}$ | Air changes per hour due to air infiltration into test room of the PASLINK test cell | [$h^{-1}$] |
| $P_e$ | Electric heating power delivered to the PASLINK test room | [W] |
| $Q$ | Heat flow rate or heat flow | [W] |
| $Q_{hfs\_t}$ | Heat flow measured by all HFS-Tiles | [W] |
| $Q_{hfs\_central}(j)$ | Heat flow measured by HFS-Tiles group (j) in the central zone of wall adjacent to the HFS-Tiles edge group (i) | [W] |
| $Q_{hfs\_edge}(i)$ | Heat flow measured by HFS-Tiles group (i) at the edge | [W] |
| $q$ | Heat Flux | [$W/m^2$] |
| $q0$ | Heat Flux value in the inner corner of the edge created by two walls | [$W/m^2$] |
| $qA, qB, qC$ | Heat Flux at measurement points A, B, C of a Multi-Tile | [$W/m^2$] |
| $T_{ext}$ | Exterior air temperature in the PASLINK emplacement | [ºC] |
| $T_{int}$ | Interior air temperature in the PASLINK test room | [ºC] |
| $\in_{ref}$ | HFS-Tiles conversion factor | [$\mu V/(W/m^2)$] |
| $\Psi$ | Linear transmission factor in a thermal bridge | [W/m·K] |

# 1. Introduction.

The calibrated absolute test cell [1] known as the PASLINK methodology [2], has demonstrated its great capacity and versatility for thermal characterization tests on building components under real dynamic external conditions [3]. Eleven countries participated in its development in a series of eight consecutive and occasionally simultaneous European projects over a decade [4][5][6]. Since its inception this methodology was raised as a standard, and therefore generated manuals that specify the requirements of the facilities as well as the procedures and analysis techniques with which their tests should be executed [7]. With this degree of definition, the PASLINK methodology can be applied regardless of the place of installation, maintaining high levels of quality in precision and reliability. This was demonstrated by the replication of an inter-comparative test called IQ-Test between different European centres equipped with PASLINK cells [8][9][10].

The initial version of this cell was the PASSYS cell, in which the heat flow through the tested sample, placed in the south face, was measured indirectly by an energy balance to the test room (see Fig 1). This balance was conducted using the difference between the interior and exterior temperatures and the power supplied to the test room [5]. The PASLINK methodology improved upon the initial design by directly measuring the heat flow using sensors called Heat Flux Sensitive Tiles (HFS-Tiles) [11] that covered the interior surfaces. Consequently, the duration of testing periods was decreased while the precision of the measured heat flow was increased. The HFS-Tiles are aluminium plates of 53x53x0.3 cm (Fig 2 left) with a 10x10x0.3 cm thermopile sensor element attached to its back face (Fig 2 centre), which generates a signal in millivolts as a function of the heat flow through the tile.

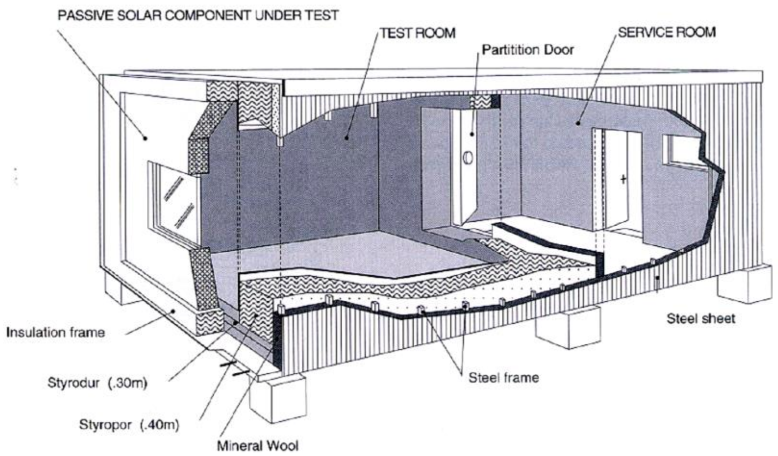


***Fig 1.*** *General structure of the PASSYS test cell [4].*

Although a PASLINK test cell envelope is built with a high level of thermal insulation on its walls, the edge effect on the conductive heat flow can not be avoided. This effect is due to the significant increase in the density of the heat flow near the inner corners, which also occurs under dynamic conditions and therefore can not be determined by a linear stationary calculation [12].

The HFS-Tiles take into account and try to quantify the edge effect using several different resources. These are connected by groups to differentiate the measurement that comes from the centre of the walls from the measurement made near the edge. The position of the sensing element on the back face of the normal HFS-Tile is not arbitrary, but is the result of analysis and simulations conducted by the designers. Some tiles, called Multi-Tiles (Fig 2 right) [13], have additional sensory elements to register the edge heat flux gradient with higher accuracy, and are strategically placed in some of the interior corners. The measurement of the edge heat flux done by the groups of HFS-Tiles along the edges can be corrected with a factor appropriately called *the edge effect Factor* $F_c$, increasing the cell's accuracy.

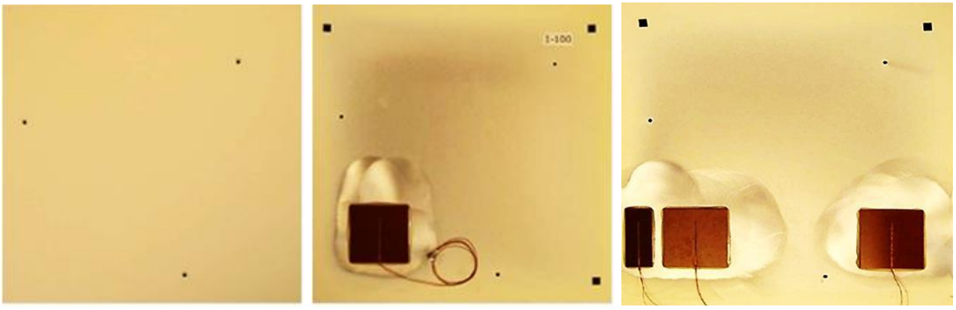

***Fig 2.*** *(From Left to Right) Front view of a normal HFS-Tile. Rear view of the same Tile. Rear view of a Multi-Tile.*

If the element to be characterized on the south face of the cell is opaque, the one-dimensional heat flow that crosses this element can be monitored with heat flux sensors installed directly in the centre and other places of the sample. If the sample is semi-transparent or very heterogeneous, the heat flow that crosses the sample can only be determined indirectly from the energy balance of the entire cell. In these cases, the precision with which the cell has been calibrated is crucial.

The calibration of a PASLINK test cell consists in the determination of the ratio between the electric heating power generated within the cell interior and the heat measured by the HFS-Tiles in the envelope of the cell. This ratio is called the total calibration factor of the cell '$F_{c\_t}$', which the PASLINK methodology accepts a maximum value of 1.2, that is, a difference of 20%. An initial test of the cell, called 'calibration test' [14], determines this total calibration factor, while the HFS-Tiles signals are verified with PASLINK network criteria, in special the groups of HFS-Tile in the edges.

A correctly constructed and monitored cell will comply with this stipulation, even without applying factors to correct edge HFS-Tile groups. However, the use of $Fc$ edge correction factors will always improve the accuracy of the cell. The PASLINK network suggests techniques to determine these factors using Multi Tile signals, and these factors remain constant in all subsequent tests. Nevertheless, the determination of these factors depends on the skill and criterion of the personal conducting the calibration test, and it is possible to have arbitrariness in this process.

This proposal suggests a method in which the edge correction factor is a dynamically determined variable from certain data measured during the execution of each test. Normally this factor remains constant and is determined only once in an initial calibration test, but with this method becomes a variable factor. The necessary correlations to apply this method are determined in an initial calibration test also, but the dynamic edge correction factors methodology have the capacity to adjust better to the heating power routines of each subsequent test. It is a more objective, impartial and reliable methodology for defining edge correction factors.

The proposed method is based on a more precise measurement of the heat flow near the edges using the instant readings collected by the Multi-Tile sensors. The validity and superiority of this method is demonstrated by the calibration test of the PASLINK test cell called EGUZKI [15][16], conducted by the working team of the Thermal Area of the Buildings Quality Control Laboratory of the Basque Government (AT-LCCE) in its facilities located in Vitoria-Gasteiz (Northern Spain). The Thermal Area staff of this laboratory set up this PASLINK test cell.

The EGUZKI Test Cell, obtained a difference of 13% in the total calibration factor of the cell $F_{c\_t}$.[17][18]. The proposed methodology reduces this difference to 6%.

Although the proposed method is obtained in the context of a PASLINK test cell, it is applicable to the correction of heat flow measurement affected by edge effect in any type of outdoor thermal characterization test in general.

It is therefore a contribution to research centres conducting outdoor tests in the two scales at which building energy performances are analysed [19]–[21]: analysis at full scale building components level or analysis at building level. At the first level, it is a contribution to at least twelve or more test facilities, research and publishing based on measurements by PASLINK test cell or similar devices [22]–[31]. At the second level, it is a contribution to more recent and bigger facilities conducting tests for energy use analysis at building level [32]–[34].

# 2. Edge effect factor determination in a PASLINK Calibration Test

## 2.1. PASLINK Test Cell Edge Effect Typologies.

The heat flow crossing the envelope of a PASLINK test cell is measured directly by HFS Tiles. These were specifically developed by the TNO Institute of the Netherlands to improve PASSYS cells [13].

A calibration test of the cell is the first task to be completed in a PASLINK facility. This test determines the degree of uncertainty between the flow measured by the HFS-Tiles and the actual flow crossing the envelope. To obtain better results, an opaque wall with the same constructive configuration as the rest of the cell, called the ‘calibration wall’, is used as a test sample on the south side. Additionally, the interior surface of this calibration wall is also covered with HFS-Tiles.

The HFS-Tiles inside the test room of the EGUZKI cell are connected in series, forming groups that differentiate the central areas of the edge zones. The Multi-tiles are strategically located in the inner corners of the cell to characterize the four types of edge effects existing in the test room (See Fig 3).

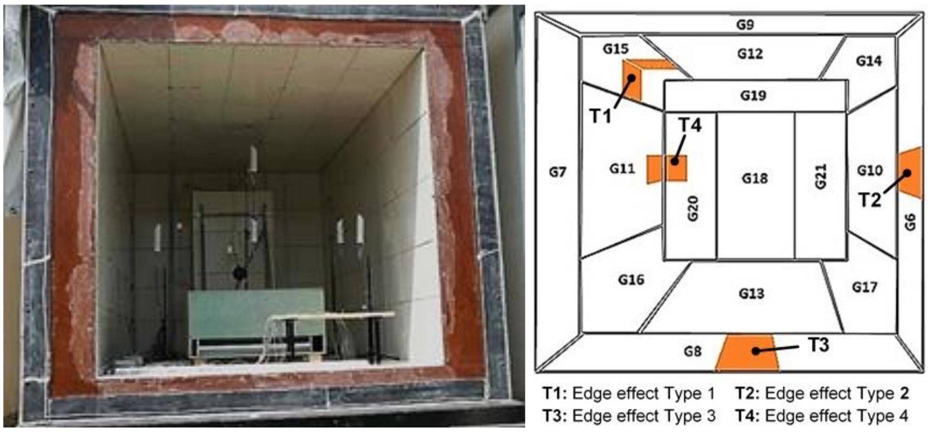


***Fig 3.*** *Test room of the EGUZKI Cell in the LCCE laboratory of Vitoria-Gasteiz and representation of the HFS-Tiles groups indicating the position of the Multi-Tiles.*

Likewise, the HFS-Tiles located over the inner surface of the calibration wall are connected forming a central group and four edge groups. The calibration wall has two edge effect types and therefore has two Multi-Tiles (See Fig 4).

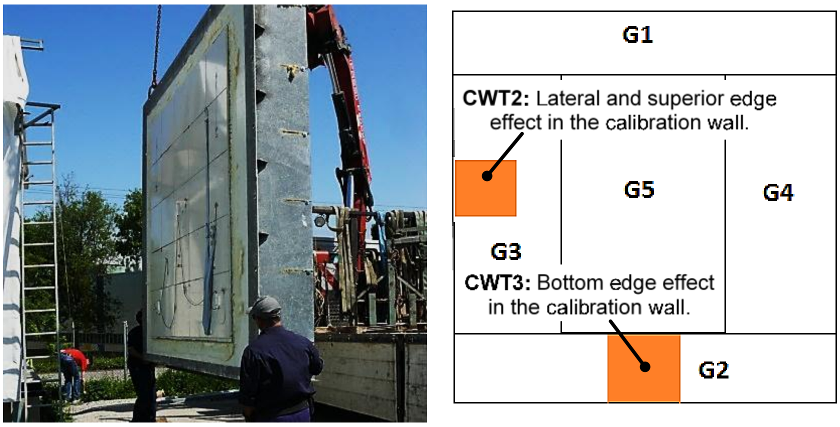


***Fig 4.*** *Calibration Wall of the EGUZKI Cell in the LCCE laboratory of Vitoria-Gasteiz and representation of the HFS-Tiles groups indicating the position of the Multi-Tiles.*

## 2.2. Edge effects treatments in a PASLINK Test.

The thermal characterization of one building element in an outdoor conditions test is associated with the balance of the heat flow in the test cell. The test room of a PASLINK acts as a calorimeter for the direct or indirect measurement of the heat flow rate fluctuations through the tested component during the test.

The HFS-Tiles measure the heat flow in the central zones of each wall of the test room accurately. On the other hand, quantifying the edge effect near the interior corners is difficult, because a high level of precision must be achieved without having a significant additional effort in instrumentation.

### 2.2.1. Edge effect estimation in the previous PASSYS Test Cell.

When the design of the first outdoor test cells was proposed it was expected to form an envelope with a completely adiabatic behaviour. This was based on the high level of insulation and the careful treatment of the structure to cancel possible thermal bridges.

In addition, the estimation of the thermal bridge from the concept of linear transmission defined in the ISO 10211 standard [35], reinforced the expectation of the adiabatic design, since very low values were obtained for the linear transmittance factors. For example, for the constructive characteristics of the EGUZKI cell of the present study, the factor obtained for the thermal bridge in the longitudinal corners of the interior of the cell, between walls and ceiling is $\Psi = 0.024$ (W/m·K).

The coefficient of linear transmittance $\Psi$ allows an estimation of the edge effect, and is useful for approximating the necessary test power. But its calculation is fundamentally a proportion of the heat flow under stationary conditions and may result in a large error in the determination of the heat flow in the edge area under dynamic conditions[35][36].

When the first cells of the PASSYS project were built and experimental tests were carried out, the importance of the edge effect was realized to be much greater than expected. Therefore, measuring edge effects with high accuracy became a crucial element to the subsequent versions of the cells.

### 2.2.2. Signal check of the HFS-Tiles edge groups.

When calibrating a PASLINK test cell equipped with HFS-Tiles, it is essential to verify that the signals obtained from the edge groups are admissible.

The signals can be verified by comparing the $Q_{hfs\text{-}edge}(i)/A(i)$ signal produced for a given group *(i)* of HFS-Tiles at the edge, with the corresponding $Q_{hfs\text{-}central}(j)/A(j)$ signal produced by the HFS-Tiles group *(j)* in the centre of the adjacent wall. This comparison must be within 1.2 ± 0.1 in the case of longitudinal edges (Typology 1), and 1.5 ± 0.2 in the case of edges at the southern end (Typologies 2 and 3) [11]. In the case of the north face (Typology 4) that corresponds to the wall separating the test room from the service room, the PASLINK methodology admits the omission of edge effect in this zone, that is, $Fc = 1$. The service room is a heated room that remains in comfort temperature conditions, reducing the effect on the test room compared to the environment outside. However, the differences between the edges and adjacent zones for the north wall also must be verified. Results within these parameters are an indication of a correctly assembled PASLINK test cell with a functional monitoring system, and without doubt such cell must produce a correct value for the total calibration factor of the cell $Fc\_t$, that is, a difference of less than 20%.

If the cell is equipped with Multi Tiles, their respective sensors *A*, *B* and *C* can be used to analyse the heat flow gradient at the edge. The signal from these sensors can also be used to determine *Fc* edge factors by using correlations between the edge flow and the one-dimensional flow. For example, the HFS-Tiles installation guide [13] suggested the correlation obtained by Rohsenow [37] to characterizes a symmetrical two dimensional corner. Another available technique is the linear approximation of the edge effect, explained below. However, as mentioned above, even when availed of these resources, the criteria and skill of the technician in charge is crucial.

#### 2.2.3. Linear approximation of the edge effect by Multi-Tile sensors.

The linear approximation of the edge effect technique is one of the main tools of the proposed method and for this reason will be briefly described.

The density of the one-dimensional heat flow in the centre of the walls corresponds directly to the measurement detected by the HFS-Tiles. Contrarily, the heat flow density near the corners has an asymptotic behaviour, which, as shown in Fig 5, can double the one-dimensional value of the central zone in only a few millimetres.

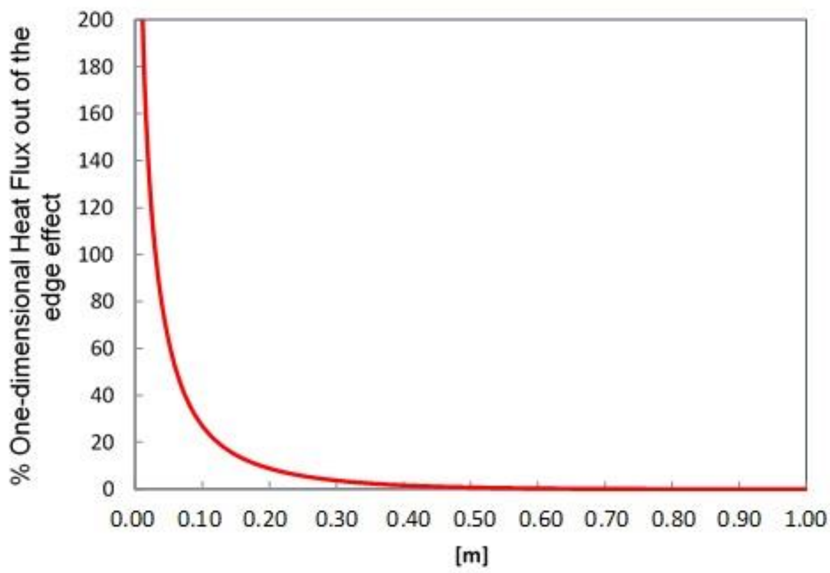


***Fig 5***. *Typical variation of heat flux near the corner due to the edge effects, expressed as percentage respect to the one-dimensional heat flux.*

The objective of the Multi-Tile is to establish the asymptotic heat flow profile during the test, at least in three of its points, as shown in Fig 6. The position of sensor *B* is strategic because it has been defined to serve as a first approximation of the average heat flux transferred at the edge through the whole HFS-Tile. The group of HFS-Tiles positioned in the edge effect area cover a length, L, measured from the corner vertex. The heat flux value $qB$ must be such that the area of the rectangle $qB \cdot L$ matches the area under the actual profile of the heat flux which corresponds to the total heat flow rate transferred by the edge.

In fact, all HFS-Tiles have their sensor element located in position *B* (12 cm from the edge of the Tile) and thus it is unnecessary to prepare separate batches for the edge and for the central zone.

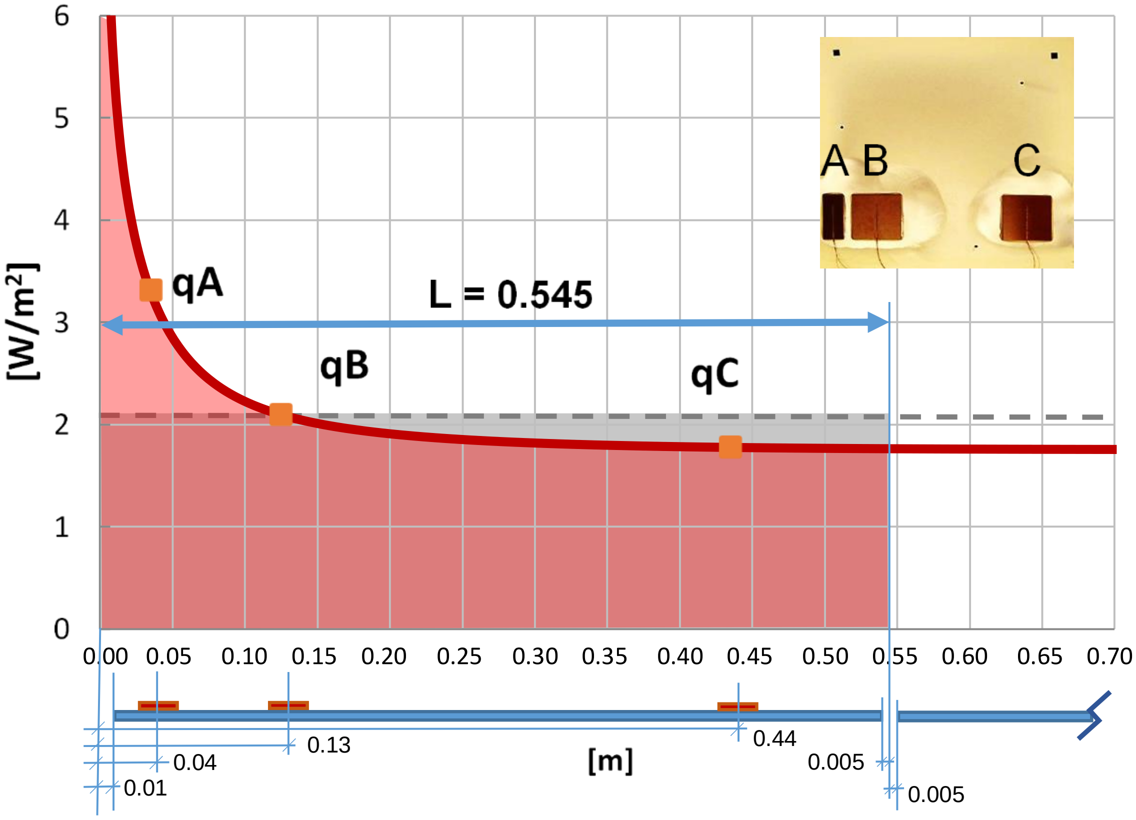


***Fig 6.*** *Sensors A (3 cm), B (12 cm), C (43 cm) of a Multi-Tile and profile of the heat flux at the edge.*

Nevertheless, the correction factor $F_c$ can be used to increase the accuracy of the total heat flux measured by sensor *B* at the edge. This is defined according to equation 1, that corresponds to the relationship between the two areas discussed.

$$F_c = \frac{\int_0^L q(x) \cdot dx / L}{qB} \quad [1]$$

The three sensors of the Multi-Tile are able to obtain a linear approximation of the function *q(x)* and therefore of the value of the integral in the equation 1.

To illustrate the linear approach procedure, the edge between roof and vertical walls, which corresponds to the edge typology T1, is taken as an example, but this analysis is valid for all edge types.

The linearization of the area under the curve of heat flow at the edge permits the approximate determination of this area. The area is determined as the sum of the polygonal areas (three triangles and three rectangles) that form the straight lines between the values *q0*, *qA*, *qB* and *qC* represented in Fig 7 and that produce the relationship indicated in equation 2.

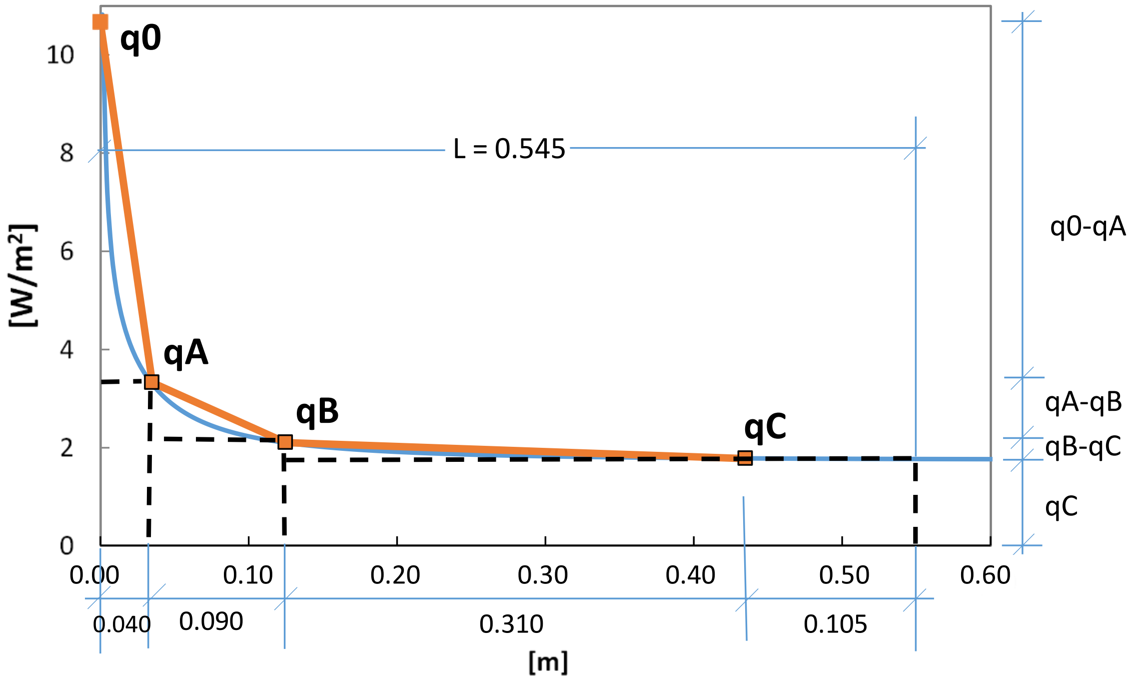


***Fig 7.*** *Linear approximation for the edge between roof and vertical walls, edge typology T1.*

$$\frac{\int_0^L q(x)\cdot dx}{L} \cong \frac{40q0 + 130qA + 400qB + 520qC}{2\cdot(10+530+5)} \qquad [2]$$

The flow values *qA*, *qB* and *qC* are measured directly by the Multi-Tile, and the value of the flow at the edge, *q0*, remains to be determined.

The value of q0 can be defined from approximations. An example is the approximation of *q0 = 6·qC* [13] for the edge effect between the vertical side wall and the south face. This is an approach established by the developers of the HFS-Tiles technique based on their studies with finite elements during the design process. This ratio is termed "*as a first guess*", because it was based on finite difference calculations for a typical structural composition of a PASLINK cell. For a particular test cell, of which its edge composition is known, a specific study with finite elements will obtain more accurate estimates of the value *q0*.

A correct estimation of the value *q0* will obtain a better linearization of the heat flow in the edge effect zone, which in turn will produce a better estimation of the correction factor $F_c$ for the reading of value *qB*. The proposed methodology is based on a finite element study for the determination of the *q0* value during the calibration test of the EGUZKI cell, as explained further. It should be noted that the simulations with finite elements included in this new methodology are a resource only used in the initial calibration test. They are not necessary for any subsequent PASLINK test conducted after calibration of the Test Cell.

## 2.3. PASLINK Test Cell Calibration Procedure.

The calibration process involves injecting a power signal of a known quantity into the test room, measuring it with a wattmeter, and comparing it to the energy measured through the envelope by the HFS-Tiles. As mentioned, a calibration wall with a thermal transmittance value similar to the envelope of the cell is used as a sample on the south face. This maximizes the accuracy of the calibration test because the flow on each surface distributes as evenly as possible.

There are three main sources of uncertainty in the measurement of the heat that crosses the envelope of the test room: the surface not covered by the HFS-Tiles, the edge effect and the heat transferred by air infiltrating into the PASLINK cell.

The measurement error due to the small separation area not covered by the HFS-Tiles is corrected by the total calibration factor of the cell.

The edge effect is detected connecting the HFS-Tiles near to the edges in separated series, independent of the HFS-Tiles wall central zone series, and by the use of correction factors *Fc* its measurement precision can be enhanced.

Air infiltration is difficult to measure in real time during the execution of the test. Therefore, the solution to this problem is to guarantee the maximum possible air tightness of the test room. In a tightly sealed cell, the effect in the balance of heat fluxes due to the transfer by infiltrated air is so low that it can also be included in the total calibration factor of the cell. The tightness of the cell is checked by measuring the level of infiltration before and after each test. The PASLINK methodology establishes that the value of renovations in the test room must be less than 0.5 $h^{-1}$ at a pressure difference of 50 Pa. In this way it is ensured that the heat exchanged per infiltration is below the measurement uncertainty of the power exchanged by the cell.

In Fig 8 the experimental data of the pressure tests before and after the calibration test of the EGUZKI cell are plotted. From this graph, it is determined that for an indoor-outdoor pressure difference of 50 Pa, the infiltrations in the test room are $n_{tr} = 0.11 \pm 0.01\ h^{-1}$ (Normal volumetric infiltration flow rate, $= 3.82 \pm 0.43\ Nm^3/h$) before the calibration test; and $n_{tr} = 0.16 \pm 0.02\ h^{-1}$ (Normal volumetric infiltration flow rate $= 5.90 \pm 0.85\ Nm^3/h$) after calibration test.

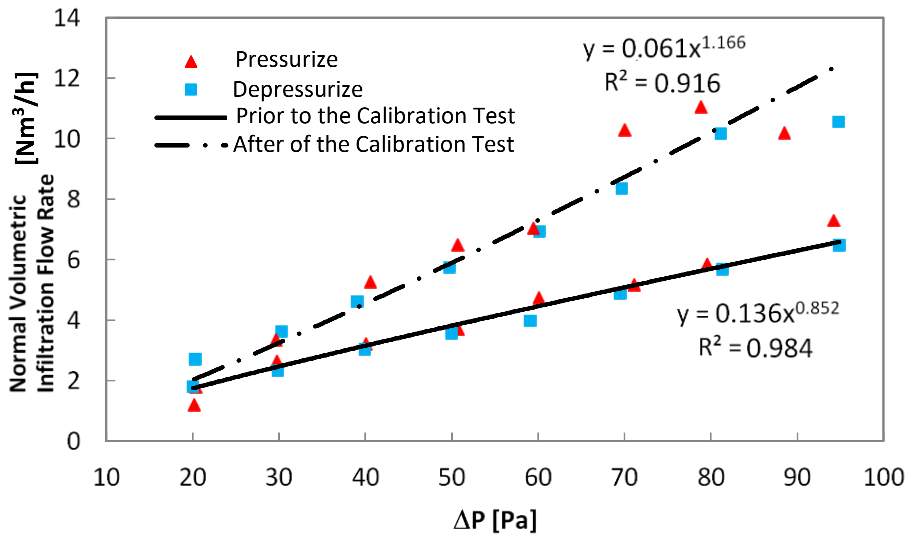


***Fig 8.*** *Measurement of air infiltration at the beginning and end of the calibration test.*

### 2.3.1. Test Routine

The goal of test procedures is to decouple and therefore differentiate the dynamic thermal response of the cell and the sample under test. To achieve this, dynamic thermal excitations of the interior of the cell are conducted through different levels and/or frequencies of electric heating power injection.

If the test cell works at different temperature levels a greater variety of results is obtained, enriching the data collected and yielding better information. Likewise, a high and variable interior-exterior temperature difference contributes to decoupling the heat gains due to the thermal difference and those due to solar gains. This method of operating the cell during a PASLINK test minimizes the duration of tests, which may require between 250 and 400 hours.

The thermal excitation of the cell is done by dynamically alternating periods of connection and disconnection of the heating electrical resistance of the test room. These periods of connection and disconnection are made following two types of temporary routine called PRBS (Pseudo Random Binary Sequence) and ROLBS (Randomly Ordered Logarithmically distributed Binary Sequence) [7]. Both routines start with an initialization period in which no heating power is applied and therefore the test temperature evolves freely. In the case of the PRBS routine, the minimum connection or disconnection interval is two hours. The minimum interval of the ROLBS routine is thirty minutes.

Fig 9 shows the typical profile of the PRBS and ROLBS routines. These have a minimum power of 50 W corresponding to the continually operating fan that maintains the indoor air in movement in order to avoid thermal stratification.

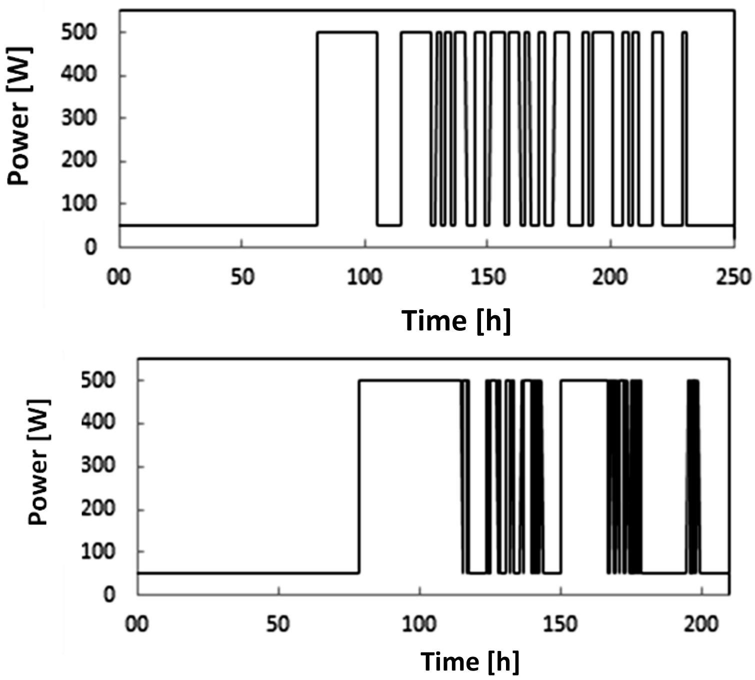


***Fig 9.*** *ROLBS routine (upper), and PRBS routine (lower).*

The calibration test performed on the EGUZKI cell consisted of two periods. The first, lasting 400 hours, consisted of the 225 hour PRBS routine, followed by 175 hours of the

ROLBS routine. The second consisted of a heating pulse applied for 300 hours with a sustained heating period during hour 101 until 200 of this phase. In all routines, the injected power was 250 W, enough to achieve indoor-outdoor temperature differences of 20 K. Fig 10 shows the evolution of the three routines used in the calibration test of the EGUZKI cell, while Fig 11 shows a detail of the high frequency period of the PRBS routine.

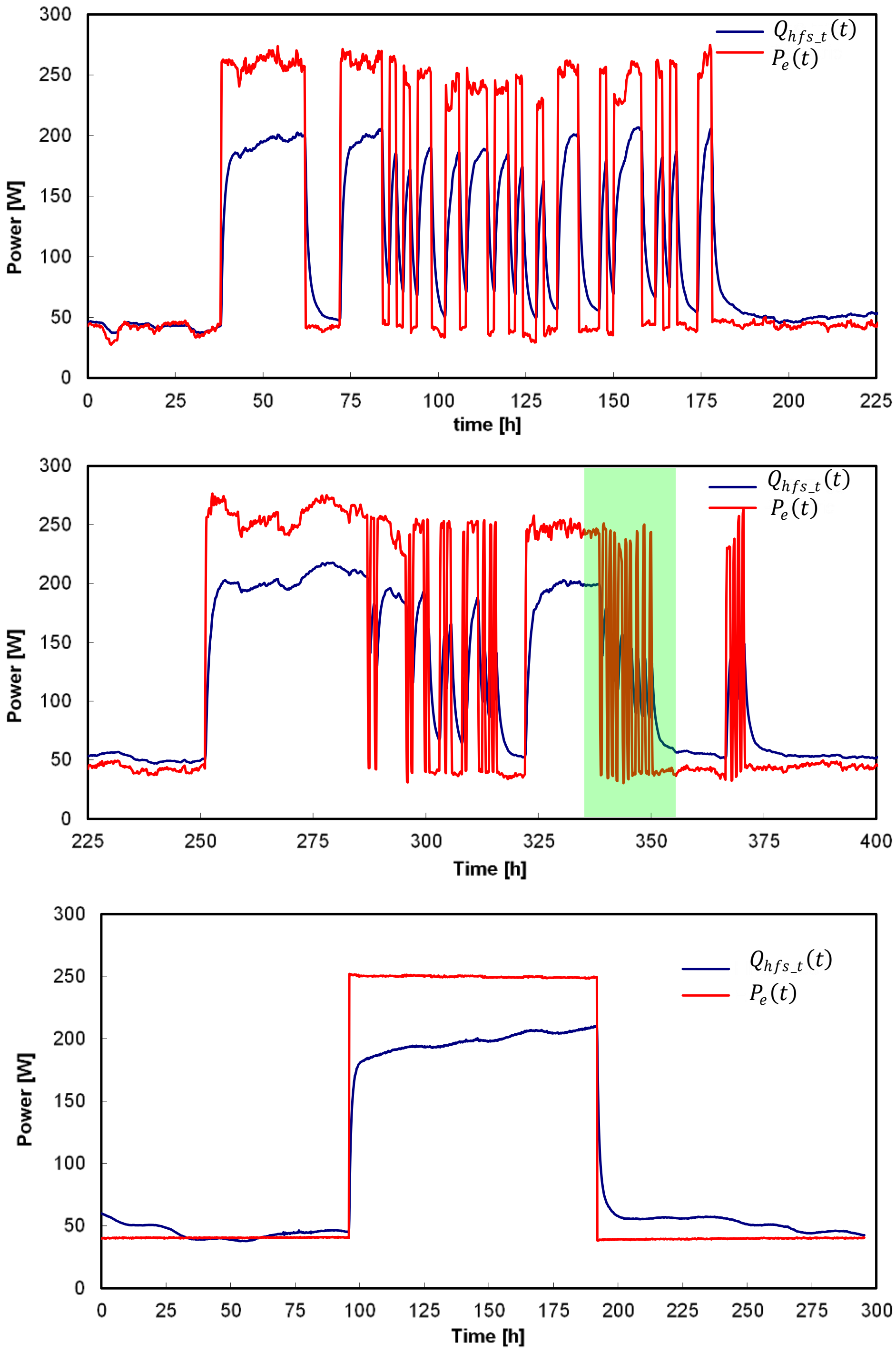


***Fig 10.*** *Electric heating power and heat flow measurement of the HFS-Tiles for the PRBS, ROLBS and PULSE routines, from top to bottom.*

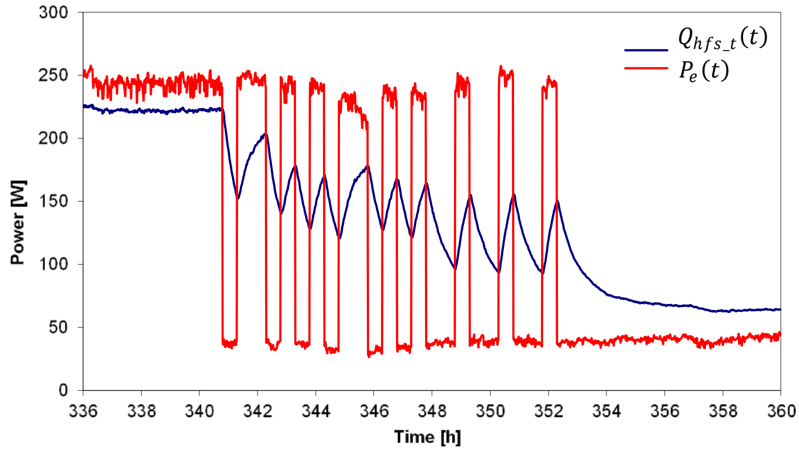


***Fig 11.*** *Response of the HFS-Tiles in a high frequency interval during the ROLBS period.*

The periods of initialization and relaxation before and after the thermal excitation of the cell must ensure that the values of the electric heating power and the total HFS-Tile are close, and also that the test cell interior air temperature registers the same value. The latter means that the test has surpassed the test cell thermal inertia. Take for example Fig 12. The temperature of the cell during the PULSE routine is verified to have reached the same value before and after the thermal excitation and this period is the reference interval to obtain the test results.

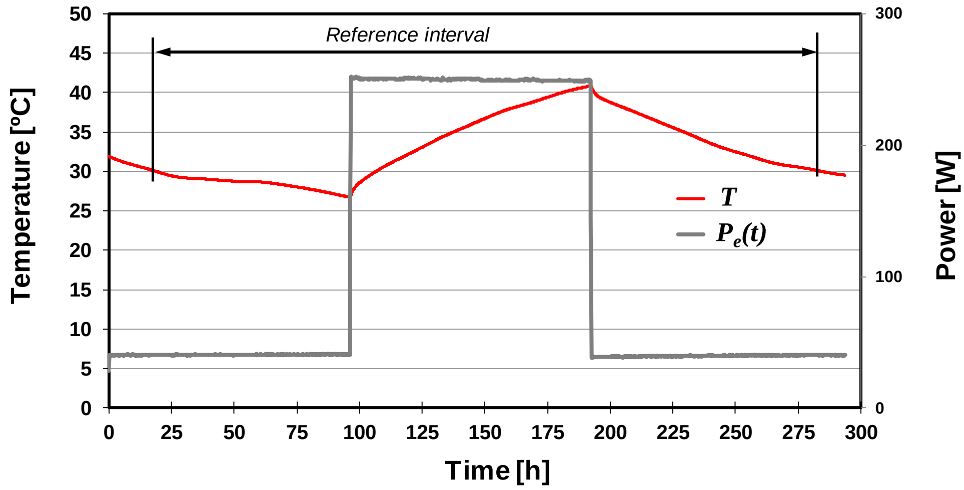


***Fig 12.*** *Graph of the test cell interior air temperature and electrical heating power during the PULSE Routine.*

### 2.3.2. Total cell calibration factor

The most important result of the calibration test is the total calibration factor of the cell '$F_{c\_t}$'. This factor represents the ratio between the time integer of the heat flow rate measured in the envelope of the test room by the HFS-Tiles '$Q_{hfs\_t}(t)$' with respect to the time integer of the electric heating power injected in the room $P_e(t)$ during the testing period (from initial test time, $t_i$, to final test time, $t_f$), and is determined according to the equation 3.

$$F_{c\_t} = \frac{\int_{t_i}^{t_f} P_e(t)dt}{\int_{t_i}^{t_f} Q_{hfs\_t}(t)dt} \quad [3]$$

A priori this factor must be greater than unity since the surface covered by the HFS-Tiles is 2.5% smaller than the total inner surface of the test room. This difference is caused by the average separation of 1 cm between each HFS-Tile. Likewise, this factor includes the effect associated with infiltrations and edge effects.

The total heat flow measured by the HFS-Tiles, $Q_{hfs\_t}$, is the sum of all groups. Each group has a certain number of HFS-Tiles that covers an area within the cell including the previously mentioned spaces between the tiles. The signal in DC voltage generated by the HFS-Tiles requires a conversion factor set at $\in_{ref}$ = 31.5 ± 1.7 µV/(W/m$^2$) at 20 ºC, with a temperature dependence of 0.14%/K. This conversion factor is recalibrated with a periodicity of 2 years. As mentioned, the measurement of the central HFS-Tile groups does not need correction, whereas the groups near the edge apply the corresponding correction factor for edge effect $F_c$ to increase the accuracy of the test cell measurement.

The total calibration factor of the EGUZKI cell is the average value of the factor obtained for the three thermal excitation routines applied.

# 3. Methodological proposal for the dynamical edge effect factor determination.

## 3.1. Hypothesis

As explained in 2.2.2., the precision of the linear approximation of heat flow near the edge (Fig 7), using the readings of Multi-Tiles (equation 2), depends on the accuracy of value *q0*.

One way of determining *q0* is by simulating the heat transfer at the cell edge using numerical models with finite volume methods. This value *q0* depends on the geometry of the edge effect and dynamic temperature conditions. The geometric and physical definition of the numerical models implicitly takes the geometrical effect into account. It is possible to analyse the dynamic effect with a dynamic simulation, using real excitations of internal and external temperatures registered during the calibration test as input. The simulation model is validated by comparing the results obtained for the heat flow and surface temperatures with those recorded in the experiment.

The next step is to determine the factors *A'*, *B'* and *C'* that solve the equality of equation 4 using numerical iteration techniques. The values of *q0*, *qA*, *qB* and *qC* are the average for the entire simulated test. The left term of this equality comes from the linear approximation (equation 2), while the term on the right allows solving the linear approximation of the edge effect without the use of *q0*.

$$40q0 + 130qA + 400qB + 520qC = A' \cdot qA + B' \cdot qB + C' \cdot qC \quad [4]$$

Finally, it is possible the dynamic determination of the correction factor *Fc*, substituting the readings from Multi-Tiles for *qA*, *qB* and *qC*, in equation 5 at each reading time interval.

$$F_c = \frac{\int_0^L q(x) \cdot dx/L}{qB} \cong \frac{A' \cdot qA + B' \cdot qB + C' \cdot qC}{2 \cdot (10 + 530 + 5) \cdot qB} \qquad [5]$$

This hypothesis is the basis of the proposed methodology for the dynamic determination of the correction factors for edge effects *Fc*. To prove its validity, Type T1 edge between the side wall and the ceiling serves as an example. The values obtained for the factors *A'*, *B*' and *C'* for each edge typology defined for the test cell are indicated in the results section.

### 3.2. Validation of the methodology proposed. Example for the roof and wall edge

In the first step, the edge of Typology 1 between a side wall and the roof was simulated using the Fluent v6.2 software. Table 1 shows the characteristics of the defined simulation model.

***Table 1.*** *Properties and Parameters of the thermal bridge model to analyse the edge effect in the edge between roof and side wall*

| | | | | | | | | | | | |
|---|---|---|---|---|---|---|---|---|---|---|---|
| **Mesh** | **Elements** | 130445 | | **Parameters** | **ΔT** | 20 | K | **Results** | **q** | 3.64 | W/m |
| | **Size** | 3 mm | | | **$U_{wall}$** | 0.070 | W/m²K | | **$L^{2D}$** | 0.182 | W/mK |
| | **EquiAngleSkew** | 0 - 0.1 | 99.61% | | **$U_{roof}$** | 0.088 | W/m²K | | **Ψ** | 0.024 | W/mK |
| | **Aspect Ratio** | 1 - 1.1 | 98.07% | | **$l_{wall}$** | 1 | m | | | | |
| | | | | | **$l_{roof}$** | 1 | m | | | | |

For a thermal difference of 20 K the simulated model produces the temperature field of Fig 13. This figure also includes the corresponding variation of the heat flux as a function of the distance from the inner corner.

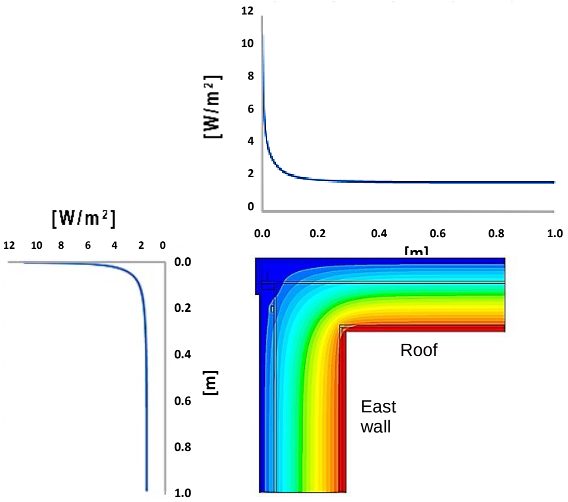


***Fig 13****. Temperature field in the section of the edge between the roof and the side wall, and profiles of the variation of the heat flux through the interior surfaces*

Likewise, for the dynamic simulation inputs are used the internal and external temperature values measured during the ROLBS routine of the calibration test, as shown in Fig 14.

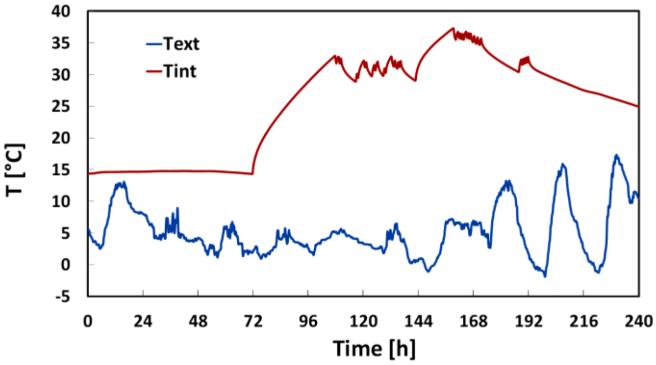


***Fig 14***. *Indoor and outdoor air temperatures recorded by the cell, applied to the numerical model of edge effect of Typology 1*

The dynamic simulation model in the area away from the edge effect produces the variation of heat fllux shown in Fig 15. The heat fluxes obtained in both the side wall and the roof are shown. Note that the values for each heat flux are very similar, affirming that both the lateral wall and roof produce the same thermal response. The PASLINK methodology considers the edge along the side walls and the roof and floor as the same type of edge, therefore the same correction factor can be applied to both.

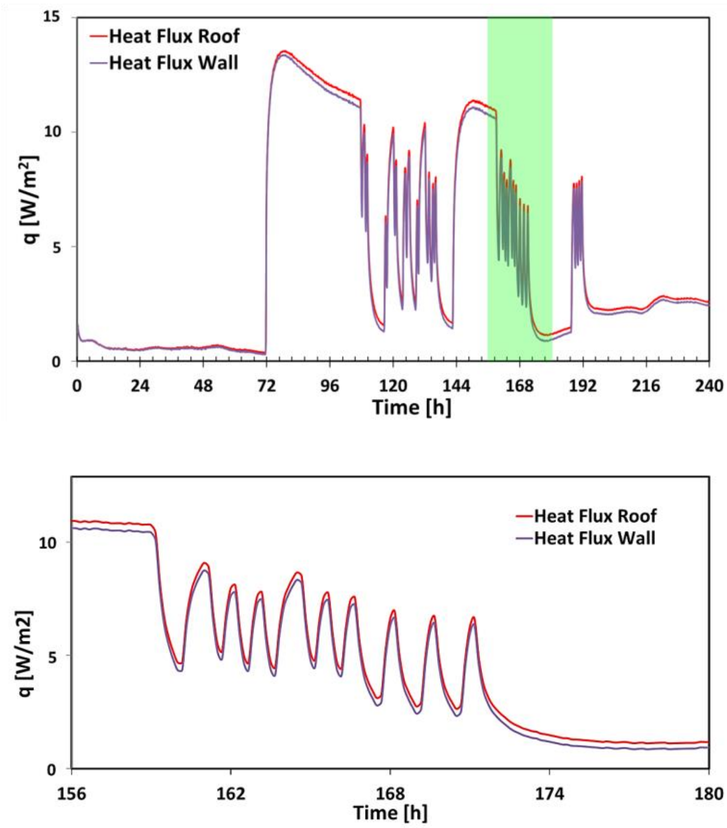


***Fig 15***. *Heat flux obtained by the numerical model in the one-dimensional heat flux area of Typology 1, the central zone of both, roof and wall. The lower figure is an amplification of the shaded interval.*

To show the variability of the heat flux gradients at the edge during the test, the analysis focuses on the time frame between 156 and 180 hours, when high frequency thermal excitation occurs and the model is subject to great variability (lower graph of Fig 15). The heat flow density versus the distance from the edge profiles are collected for hours 156, 162, 168, 174 and 180. These hours cover instants before, during and after the thermal excitation. The profiles obtained during these times are shown in Fig 16. A greater gradient is verified for the moments of greater heating power, as well as the correspondence of *qC* with the one-dimensional flow further from the edge.

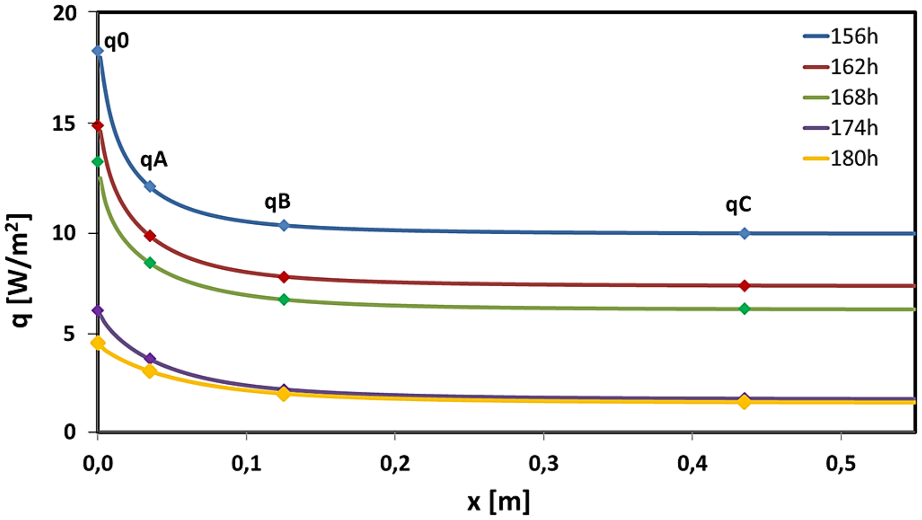


***Fig 16***. *Variation of the profile of the heat fluxes for the edge effect of Typology 1. The values were obtained from different moments during the test simulation.*

Second, the difference between results obtained by the simulation and the data collected in the test was checked. The maximum difference was found to be less than 15%. Therefore, the simulation was considered valid.

Third, it is necessary to determine the factors *A'*, *B'* y *C'*. In the given example, the iteration process to solve equation 4 produces the following values: *A'*=290.20, *B'*=368.13 and *C'*=609.18.

With the proposed method, the magnitude of the factor *Fc* varies according to the value of the heat flux measured by HFS-Tiles and this variation allows an adjustment adapted to the level of this particular heat flux. This is to be expected, considering that dynamic factors have been defined as a function of the heat flux gradient at the edge. In contrast, the constant correction factor of the original PASLINK method, amplifies the HFS-Tiles signal equally throughout the test, reducing the measurement error during high heating power periods but increasing it during low power periods.

Fig 17 shows the adjustment of the HFS-Tiles signal for the calibration test in the case of PULSE and ROLBS routines, applying dynamic correction factors in all edge groups (except the north wall). The adjustment of the dynamic edge effect correction factors performs differently in periods of low and high heating power.

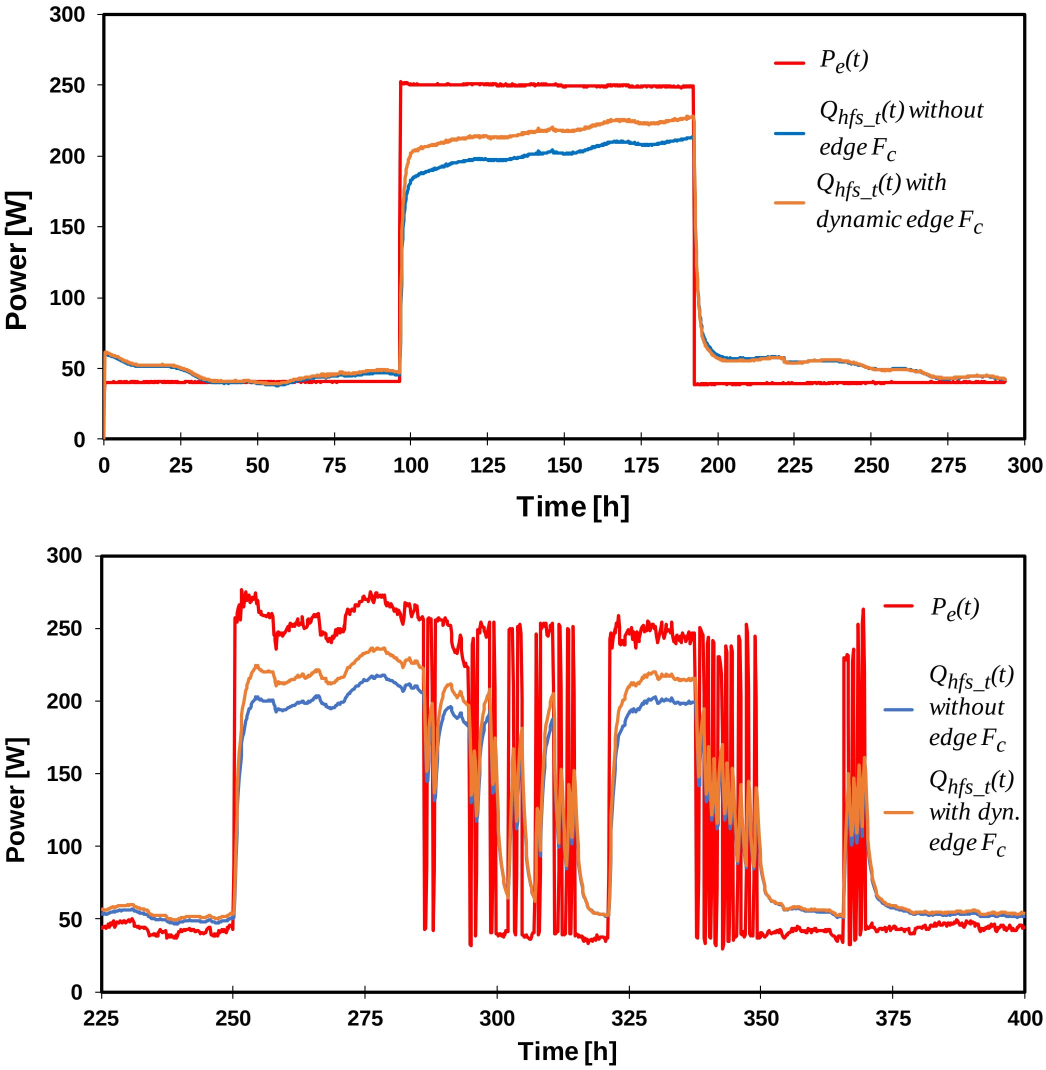


***Fig 17.*** *Comparison of the signal of HFS-Tiles with and without edge effect corrections through dynamic factors for the PULSE (Top) and ROLBS (Bottom) routines.*

In summary, the proposed methodology establishes the following steps for the determination of the edge effect correction factor:

- Make a model of finite elements from the geometry and properties of the edge components to be characterized.
- Simulate the edge dynamically for an extended period of time, preferably higher than the estimated time constant for the model, using the measurements recorded in the calibration test as thermal boundary conditions.
- Check the adjustments of the values measured by the sensor elements for heat fluxes *qA*, *qB*, and *qC* compared to the simulation. In this stage it is also possible to check that the distance of the edge considered by the model covers the edge effect zone completely.

- If the adjustment between the simulation and measured data is not correct, the information used to create the simulation model, whether geometrical or physical properties, must be reviewed and the dynamic simulation repeated.

- From the average values of *q0*, *qA*, *qB* and *qC* obtained from the test simulation, determine by iteration the factors *A'*, *B'* and *C'* that allow generating the equivalent function for the linear approximation of the edge effect omitting the term *q0* (equation 5).

- Use the function obtained to calculate the edge correction factor $F_c$ at each time interval of the experimental readings recorded by the Multi-Tiles for *qA*, *qB* and *qC*. This procedure is repeated for every type of edge to be considered.

# 4. Results.

## 4.1. Test Cell total calibration factor using the PASLINK signal verification procedure

The total calibration factor of the EGUZKI cell using the signal of the HFS-Tile groups, without edge effect correction factors, and making the signals check indicated by the PASLINK methodology as described in section 2.2.3, and using three different routines has been:

$F_{c\_t}|_{PULSE}$ = 1.12 for the PULSE routine [18], $F_{c\_t}|_{PRBS}$ = 1.15 for the PRBS routine and $F_{c\_t}|_{ROLBS}$ = 1.13 for the ROLBS routine. Therefore the final value for the total calibration factor of the EGUZKI cell obtained has been: $F_{c\_t}$ = 1.13 ± 0.02 [17].

The PASLINK methodology supports a maximum value of 1.2 for this factor. The value obtained is indicative of the EGUZKI cell's high quality. However, this precision can be increased even more as illustrated in the following results, obtained with the new proposed methodology

## 4.2. Test Cell Total Calibration factor using dynamical edge effect factor determination

The process described in section 3.2 is repeated for the other edge effect typologies: T2 edge between the lateral walls or the roof of the test room with the south wall; T3 edge between the floor of the test room and the south wall (see Fig 3); CWT2 edge between the lateral and superior sides of the calibration wall with the test cell; CWT3 edge between the bottom side of the calibration wall with the test cell floor (see Fig 4).

Although the calibration wall has a constructive composition similar to the longitudinal walls of the test cell, the heat flow crossing this calibration wall differs from the heat flow crossing the walls of the cell. This is due to its smaller area and the geometric and material change caused by the frame holding the calibration wall fixed to the cell. For this reason, the calibration wall considers both edge effect typologies: CWT2 and CWT3.

In the case of Typology 4, located in the north wall of separation between the test room and the service room, the correction factor is taken as the unit $F_c$=1, as noted earlier.

Fig 18 shows the temperature field and the heat flux profiles on the interior surface obtained in the junction zone between the east wall and the calibration wall (zone of T2 and CTW2), while Fig 19 shows the same for the edge in the floor zone (zone of T3 and CWT3).

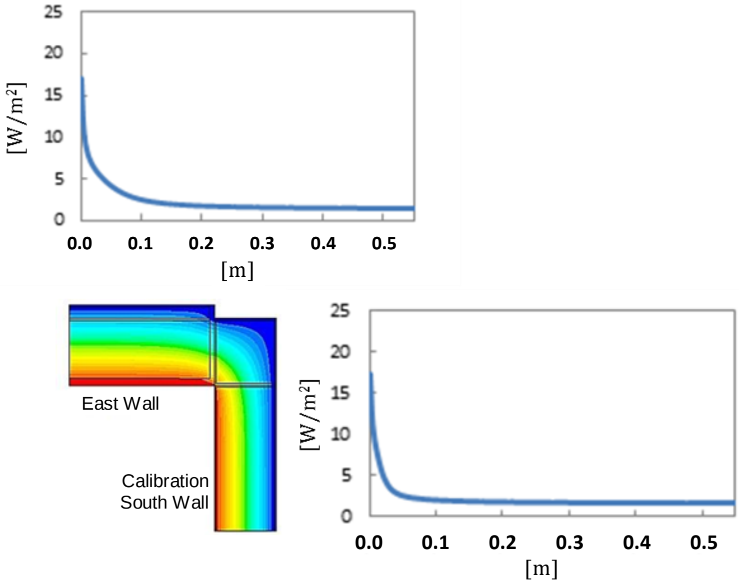


***Fig 18.*** *Edge simulation model of Typology 2 with the corresponding inner surface heat flux profiles.*

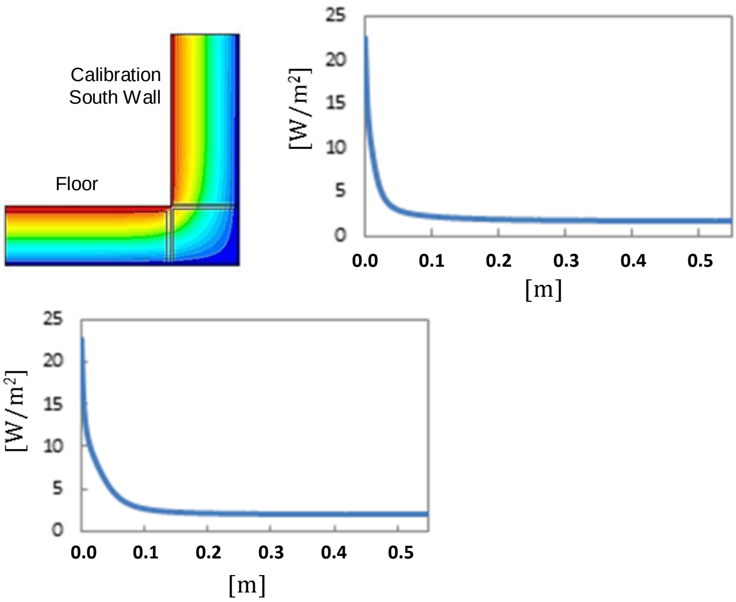


***Fig 19****. Edge simulation model of Typology 3 with the corresponding inner surface heat flux profiles.*

The heat fllux is slightly higher in the floor area of the calibration wall than in the ceiling zone because of the difference in materials and thickness of the insulation used within the frame upper and lower parts.

The correction factors in the calibration wall CWT2 and CWT3 allow the adjustment of the heat measurement that effectively crosses this component and are crucial for both determining the total factor of calibration of the cell and in later lumped parameter modelling of the calibrated cell.

The edge effects of typologies 1 and 4 are typical phenomena of the cell structure. In the case of typologies 2 and 3 at the southern opening of the test room, the effects will depend in part on the characteristics of the sample. The calibration wall is the PASLINK test sample with the highest possible level of insulation and therefore it is the sample that has the greatest edge effect on typologies 2 and 3.

Consequently, the correction factor in the HFS-Tile groups at the south opening can overestimate the edge effect when the cell is testing other components that are not the calibration wall. The technique proposed, based on the instantaneous reading provided by the Multi-Tiles, will be less exaggerated in its overestimation than if a constant value is used for $F_c$ from the calibration test.

Applying the methodology described, the correlations collected in Table 2 and Table 3 have been obtained for the interior of the test room and in Table 4 for the calibration wall. These correlations enable the dynamic calculation of correction factors of the edge effect Fc for every edge effect type.

***Table 2.*** *Correlation obtained of the correction factor of long sides of the test cell. Edge effect Type 1.*

| *Factor Type* | *Correlation* |
|---|---|
| $F_{c(T1)}$ | $\frac{290.20 \cdot qA + 368.13 \cdot qB + 609.18 \cdot qC}{1090 \cdot qB}$ |

***Table 3.*** *Correlation obtained of the correction factor of the south side of the cell. Edge effect Types 2 and 3.*

| *Factor Type* | *Correlation* |
|---|---|
| $F_{c(T2)}$ | $\frac{176.17 \cdot qA + 367.77 \cdot qB + 867.36 \cdot qC}{1090 \cdot qB}$ |
| $F_{c(T3)}$ | $\frac{360.72 \cdot qA + 381.14 \cdot qB + 596.43 \cdot qC}{1090 \cdot qB}$ |

***Table 4.*** *Correlation obtained of the correction factor in calibration wall. Edge effect Types CWT2 and CWT3.*

| *Factor Type* | *Correlation* |
|---|---|
| $F_{c(CWT2)}$ | $\frac{175.88 \cdot qA + 367.57 \cdot qB + 867.19 \cdot qC}{1090 \cdot qB}$ |
| $F_{c(CWT3)}$ | $\frac{294.47 \cdot qA + 340.14 \cdot qB + 562.40 \cdot qC}{1090 \cdot qB}$ |

Finally, the final calibration value of the cell obtained as the average of three repetitions of the calibration test, using different routines of excitation of the cell each time, and correcting the readings of the heat flow made by the HFS-Tiles edge groups with dynamic factors, is:

$$\boldsymbol{F_{c\_t} = 1.06 \pm 0.02}$$

Therefore, in the case of the EGUZKI Test cell, the measurement error of the heat transferred through its envelope is reduced from 13% to 6% by applying this new methodology. This is a 54% error reduction on the energy balance carried out during the PASLINK tests.

## 5. Conclusions.

The PASLINK methodology has proven to be a highly reliable technique for the thermal characterization of building components under outdoor testing conditions, as shown by the intercomparability tests carried out during its development.

The total calibration factor of the EGUZKI cell determined with actual PASLINK methodology indicates that the uncertainty in the measurement made by the HFS-Tiles for the heat flow that crosses the envelope of the cell is 13%. This value is indicative of the EGUZKI cells high quality. However, the dynamic edge effect factor determination has shown to further reduce this uncertainty by a 54%.

The proposed method is based on a combination from the readings of the heat flux sensors located in the Multi-Tiles, together with simulations of the edges of the test cell. This is a resource only used in the initial calibration test. The correlations obtained to determine the Fc factors in function of the Multi-Tile readings in this initial calibration test are valid for any subsequent PASLINK test.

Dynamic edge effect correction factors have been demonstrated to be an adaptive technique based on the heat flux level through the envelope, increasing the adjustment in periods of high heat flow and making little adjustment in periods of low heat flow. In contrast, the adjustment provided by a constant edge correction factor amplifies the value proportioned by the HFS-Tile signals, both in periods of low and high heat flow through the envelope, reducing the error in periods of high heat flow but increasing it in periods of low heat flow. In the case of the southern edges of the cell, a constant edge correction factor can produce overestimations of the adjusted heat flux, while a dynamic factor helps to prevent this.

The dynamical edge effect factor determination methodology has shown itself to be an objective, impartial and reliable technique to define edge effect correction factors.

Any outdoors or in-situ characterization technique with tests based on the measurement of heat flux can apply the proposed methodology to determine the edge effect correction during dynamic tests. For this, at least three heat-flow sensing elements are required and must be arranged in a configuration similar to that of a Multi-Tile. The capability to numerically simulate any given edge is also necessary. With the sensor readings and the simulation results, the correlations for the edge effect factor determination can be obtained. This determination is only necessary once during the calibration test.

## Acknowledgments.

This project has been made possible thanks to the agreement between the Basque Government and the University of the Basque Country UPV / EHU through of the ENEDI research group for the management and development of the Thermal Area of the Buildings Quality Control Laboratory of the Basque Government (AT-LCCE). This work was supported by the Spanish Ministry of Science, Innovation and Universities and the European Regional Development Fund through the MONITHERM project, reference: RTI2018-096296-B-C22 (MCIU/AEI/FEDER, UE).

The set-up of the PASLINK cells at the AT-LCCE facilities in Vitoria-Gasteiz has been successfully completed, thanks to the advice and support of Mr. Hans Bloem of the DYNASTEE group.

## References.

[1] G. Cattarin, F. Causone, A. Kindinis, and L. Pagliano, "Outdoor test cells for building envelope experimental characterisation – A literature review," *Renew. Sustain. Energy Rev.*, vol. 54, pp. 606–625, 2016.

[2] P. H. Baker and H. A. L. van Dijk, "PASLINK and dynamic outdoor testing of building components," *Build. Environ.*, vol. 43, no. 2, pp. 143–151, Feb. 2008.

[3] P. a. Strachan and P. H. Baker, "Editorial - Outdoor testing, analysis and modelling of building components," *Build. Environ.*, vol. 43, no. 2, pp. 127–128, 2008.

[4] L. Vandaele and P. Wouters, "The PASSYS Services, Summary Report. BBRI and EC DG XII. EUR 15113 EN.," Brussels, EUR 15113 EN, 1994.

[5] H. A. L. A. L. Van Dijk and G. P. P. Van der Linden, "The PASSYS method for testing passive solar components," *Build. Environ.*, vol. 28, no. 2, pp. 115–126, 1993.

[6] T. F. van Dijk HAL, "Final report of the JOULE II COMPASS Project (JOU2-CT92-0216)," 1995.

[7] H. A. L. Van Dijk and F. Tellez, "COMPASS Measurement and data analysis procedures," Brussels, JOULE II - COMPASS, 1995.

[8] L. Vandaele, P. Wouters, and H. Bloem, "IQ-test - Improving quality in testing and evaluation of solar and thermal characteristics of building components," in *23rd AIVC and EPIC 2002 Conference*, 2002, pp. 853–858.

[9] P. Baker, "IQ-test—improving quality in testing and evaluation of solar and thermal characteristics of building components," *Energy Build.*, vol. 36, no. 5, pp. 435–441, 2004.

[10] P. H. Baker, "Evaluation of round-robin testing using the PASLINK test facilities," *Build. Environ.*, vol. 43, no. 2, pp. 181–188, Feb. 2008.

[11] H. A. L. Van Dijk and F. Van Der Graaf, "Research report HFS Tiles for the Passys Test Cells," TNO Building and Construction Research, Delft, 1994.

[12] K. Martin, A. Erkoreka, I. Flores, M. Odriozola, and J. M. Sala, “Problems in the calculation of thermal bridges in dynamic conditions,” *Energy Build.*, vol. 43, no. 2–3, pp. 529–535, 2011.

[13] G. P. Van Der Linden, H. A. L. Van Dick, A. J. Lock, and F. Van Der Graaf, “COMPASS Installation guide HFS tiles for the PASSYS test cells,” Brussels, JOULE II - COMPASS, 1995.

[14] B. Saxhof, “Paslink Calibration Manual,” Brussels, JOULE II - COMPASS (A revision of the PASSYS calibration manual. ed. B. stanzel, ITW university of stuttgart. EUR 15120 EN), 1995.

[15] A. Erkoreka, “Eguzki and Ilargi PASLINK test cells, LCCE Vitoria-Gasteiz, Spain,” in *Full scale test facilities for evaluation of energy and hygrothermal performances. International Workshop*, INIVE EEIG, Ed. Brussels, 2011, pp. 51–62.

[16] C. García-Gáfaro, A. Erkoreka, C. Escudero-revilla, I. Flores, J. Martínez-fontecha, and J. M. S. Lizarraga, “Experience gained in the Thermal Characterization of Building Components by using Paslink Test Cells,” in *Proceedings of the 5th IBPC*, 2012, pp. 331–338.

[17] C. Escudero-Revilla, “Caracterización Experimental del Comportamiento Energético de Fachadas Ventiladas (Outdoor Test for Thermal Characterization of Ventilated Facades),” Phd Thesis (In Basque and Spanish Lang.). Thermal Engineering Department - ENEDI Group. University of the Basque Country UPV/EHU, Bilbao, Spain. 2016.

[18] S. J. M. Erkoreka A., Escudero C., Flores I., Garcia C., “Upgrading and calibration of two PASLINK test cells. Evaluation through the ‘IQ-TEST’ round- robin test,” in *DYNASTEE workshop on Dynamic Methods for Building Energy Assessment*, 2010.

[19] A. Janssens, *Inventory of full scale test facilities for evaluation of building energy performances*. KULeuven, 2016.

[20] S. Roels, “Annex 58 Project Summary Report - Reliable Building Energy Performance Characterisation Based on Full Scale Dynamic Measurements,” Wimbledom, London, UK., 2017.

[21] A. Janssens, S. Roels, and L. Vandaele, *Full Scale Test Facilities for Evaluation of Energy and Hygro thermal Performance*. INIVE-DYNASTEE International Workshop, Brussels, 2011.

[22] F. Ochs, D. Siegele, G. Dermentzis, and W. Feist, “Prefabricated Timber Frame Façade with Integrated Active Components for Minimal Invasive Renovations,” *Energy Procedia*, vol. 78, pp. 61–66, 2015.

[23] H. Hens, A. Janssens, W. Depraetere, J. Carmeliet, and J. Lecompte, “Brick Cavity Walls: A Performance Analysis Based on Measurements and Simulations,” *J. Build. Phys.*, vol. 31, no. 2, pp. 95–124, Oct. 2007.

[24] T. Z. Desta, J. Langmans, and S. Roels, “Experimental data set for validation of heat, air and moisture transport models of building envelopes,” *Build. Environ.*, vol. 46, no. 5, pp. 1038–1046, May 2011.

[25] W. Maref, M. A. Lacasse, and D. G. Booth, “Large-scale laboratory measurements and benchmarking of an advanced hygrothermal model,” in *CIB 2004 Conference: 02 May 2004, Toronto, Ontario*, pp. 1–11.

[26] M. Liu, K. B. Wittchen, and P. K. Heiselberg, “Verification of a simplified method for intelligent glazed façade design under different control strategies in a full-scale façade test facility – Preliminary results of a south facing single zone experiment for a limited summer period,” *Build. Environ.*, vol. 82, pp. 400–407, Dec. 2014.

[27] S. Pinard, G. Fraisse, C. Ménézo, and V. Renzi, “Experimental study of a chimney enhanced heat emitter designed for internal renovation of buildings,” *Energy Build.*, vol. 54, pp. 169–178, Nov. 2012.

[28] G. Alcamo, “Daylight distribution and thermo-physical evaluation of new facade components through a test cell for the overheating control in Mediterranean Climate,” in *Proceedings of the 5th international conference SOLARIS*, 2011.

[29] M. J. Jiménez, B. Porcar, and M. R. Heras, “Estimation of building component UA and gA from outdoor tests in warm and moderate weather conditions,” *Sol. Energy*, vol. 82, no. 7, pp. 573–587, 2008.

[30] M. J. Jiménez, B. Porcar, and M. R. Heras, “Application of different dynamic analysis approaches to the estimation of the building component U value,” *Build. Environ.*, vol. 44, no. 2, pp. 361–367, Feb. 2009.

[31] S. Martínez, A. Erkoreka, P. Eguía, E. Granada, and L. Febrero, “Energy characterization of a PASLINK test cell with a gravel covered roof using a novel methodology: Sensitivity analysis and Bayesian calibration,” *J. Build. Eng.*, vol. 22, pp. 1–11, Mar. 2019.

[32] L. Bianco, P. Schneuwly, E. Wurtz, and A. Brun, “Design of a New Full-scale Facility for Building Envelope Test: FACT (FACade Tool),” *Energy Procedia*, vol. 111, pp. 256–266, Mar. 2017.

[33] F. Alzetto, D. Farmer, R. Fitton, T. Hughes, and W. Swan, “Comparison of whole house heat loss test methods under controlled conditions in six distinct retrofit scenarios,” *Energy Build.*, vol. 168, pp. 35–41, Jun. 2018.

[34] Danish Technological Institute, “EnergyFlexHouse.” [Online]. Available: https://www.dti.dk/labs/energyflexhouse/technology-to-the-global-challenge/25348. [Accessed: 01-Jun-2019].

[35] EN ISO 10211:2012, *Thermal bridges in building construction - Heat flows and surface temperatures - Detailed calculations*. .

[36] K. Martin, A. Campos-Celador, C. Escudero, I. Gómez, and J. M. Sala, “Analysis of a thermal bridge in a guarded hot box testing facility,” *Energy Build.*, vol. 50, pp. 139–149, 2012.

[37] W. M. Rohsenow, J. P. Hartnett, and Y. I. Cho, *Handbook of heat transfer*. McGraw-Hill, 1998.